ACS PHYSICAL CHEMISTRY Au
AN OPEN ACCESS JOURNAL OF THE AMERICAN CHEMICAL SOCIETY

pubs.acs.org/physchemau
Letter

Choreoisosteres: Pseudoatom Variation in Macrocyclic Hinges Conserves Structure and Dynamics

Alexander J. Menke, Joseph H. Reibenspies, Casey J. Patterson-Gardner, Alexander M. Engstrom, R. Scott Lokey, and Eric E. Simanek*

Cite This: ACS Phys. Chem Au 2025, 5, 134−138
Read Online
ACCESS | Metrics & More | Article Recommendations | Supporting Information

ABSTRACT: Differing in pseudoatom, three macrocycles with isosteric substitutions (geminal dimethyl, cyclopropyl, cyclobutyl) can be described as choreoisosteres. Under ambient conditions, they share a dynamic hinge-like motion that can be described as fully revolute in solution. The barriers to hinging, $\Delta G^{\ddagger}$, are identical within experimental error: $\Delta G^{\ddagger}$ = 14.2−15.2 kcal/mol as judged by variable-temperature ^{13}C NMR spectroscopy. Consistent with conserved dynamic behavior and isosterism, other physical properties including hydrophobicity and solution/membrane diffusion constants are amenable to prediction.

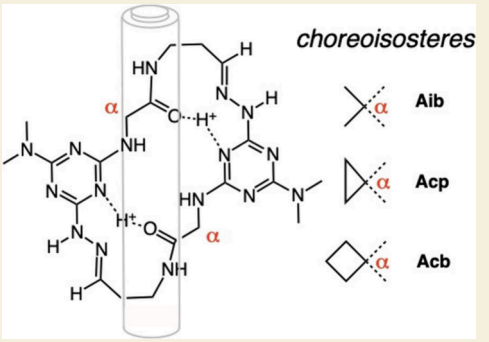

KEYWORDS: *isostere, macrocycle, dynamics, hinge, triazine*

Writing from the Research Laboratory of the General Electric Company in 1919, Langmuir defined *isosteres* narrowly, requiring molecules (or ions) to have identical numbers of valence electrons, and accordingly, equivalent numbers of atoms.[1] Through this lens, isosteres varied either by atom choice (carbon monoxide and nitrous oxide) or by charge (H^- and He). Langmuir argued that the "physical properties of [N_2/CO and CO_2/N_2O] furnish proof of the similarity of structure predicted by the octet theory, and show the usefulness of the conception of isosterism." Facilitating prediction motivated Langmuir's efforts.

In 1925, Grimm loosened Langmuir's definition of isosterism to include *pseudoatoms*. With -CH- and nitrogen defined as a pseudoatoms, isopropyl and dimethylamino groups became isosteres.[2] In 1933, Erlenmeyer extended this concept further, identifying -S- and -C═C- as isosteric, conveying this distinction to thiophene and benzene.[3] Historically, *isostere* was a descriptor primarily reserved for functional groups.

When, in 1951, Friedman introduced *bioisosterism*, the isostere distinction transcended from functional groups to molecules.[4] In addition to meeting the atomic (or pseudoatomic) equivalency requirement, *bioisosteres* were defined as molecules that shared a common property−similar biological activity. That is, one could predict that substituting a cyclopropyl ring for an isopropyl group should convey similar biological activity while allowing a secondary property to be subtly tuned to improve pharmacokinetics or pharmacodynamics.[5]

Yet, molecular isosterism need not be limited to biological activity. Here, we define *choreoisosteres* as molecules that meet the definition of isosteres *and* demonstrate similar dynamic behavior. Chart 1 shows three macrocycles containing isosteric groups comprising recognizable pseudoatoms: geminal dimethyls (**Aib**), cyclopropyl rings (**Acp**), and cyclobutyl rings (**Acb**).[6,7] These macrocycles behave as molecular mortise (door) hinges and undergo fully revolute dynamic motion.[8,9] To meet the conditions of choreoisosterism, we show that these macrocycles (i) are isomorphous in both solid state and solution by virtue of pseudoatom substitution, (ii) undergo common, hinge-like motion, and (iii) have additional physical properties that are shared, a surrogate for the predictive ability conveyed by this distinction. Indeed, predictive ability formed the foundation for the arguments advanced by Langmuir, Grimm and Friedman.

CRYSTALLOGRAPHY REVEALS THE MOLECULES ARE ISOMORPHIC IN THE SOLID STATE

Figure 1 shows the solid-state structures obtained for **Aib**, **Acp** and **Acb**. All three adopt a closed hinge geometry in the solid state. The pseudoatoms of one subunit are indicated in circles.

Received: December 9, 2024
Revised: February 7, 2025
Accepted: February 11, 2025
Published: March 10, 2025

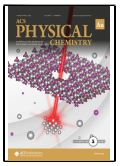

Chart 1. Choreoisosteres[a]

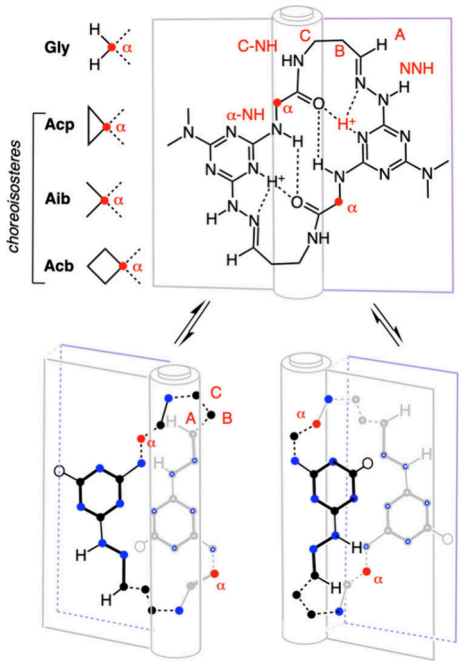

[a]Hinge-like motion interconverts enantiomers. Chemical exchange upon hinging occurs at α, B, and C. NMR labels are shown in red. The dimethylamine groups are shown as circles to guide the eye. Line weight reflects rigidity.[10] Adapted from Ref 11 with permission from the Royal Society of Chemistry.

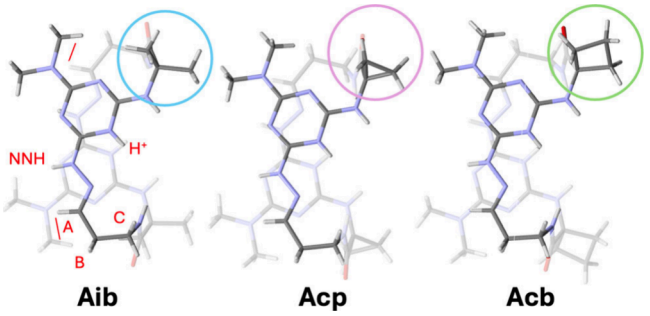

Figure 1. Crystal structures of **Aib**, **Acp**, and **Acb**. The pseudoatom sites are identified with circles. Colors correspond to resonances in Figure 4. The red lines on **Aib** shows a critical rOe (A to the dimethylamine group) that establishes hinge structure in solution for each macrocycle.

The extended π-systems comprising the hinge leaves are flush upon each other. The macrocycles orient the amide carbonyl outward. Rotation of the carbonyls inward provides bifurcated hydrogen bonding with α-NH and H^+, a network that is attributed as the basis of quantitative cyclization.[12,13]

An overlay of the macrocycle backbones (Figure 2) confirms conservation of structure and reveals slight variations in the nature of the overlap that are reflected in the ^{1}H NMR spectra.

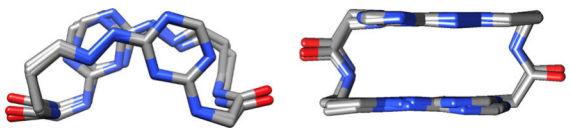

Figure 2. Backbone overlap of the solid state structures.

NMR SPECTROSCOPY REVEALS THAT THE MOLECULES ARE ISOMORPHOUS IN SOLUTION

Figure 3 shows the fingerprint region of the ^{1}H NMR spectrum of these macrocyles. The chemical shifts confirm hydrazone

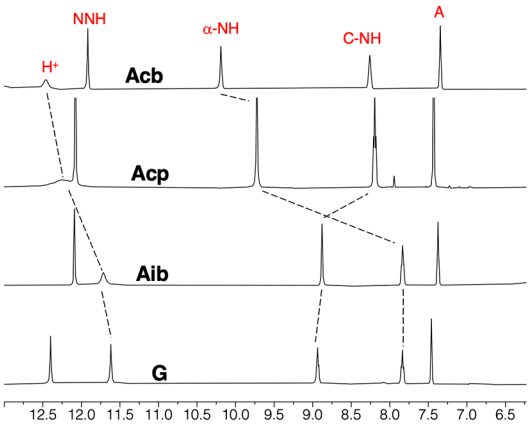

Figure 3. Fingerprint regions of the 400 MHz ^{1}H NMR in DMSO-d_6 showing symmetry across the subunits and chemical shifts consistent with hydrogen bonding.

formation (A), protonation (H^+) and hydrogen bonding (downfield shifts of C-NH, α-NH).[9] Symmetry in these molecules is reflected by the single set of resonances corresponding to both subunits. Access to the closed hinge is confirmed by rOes: the dimethylamine group of one leaf is brought into proximity with the hydrazone (A) of the other leaf in this geometry. This rOe is shown as with red lines in the crystal structure of **Aib** (Figure 1). The marked differences in chemical shifts associated with α-NH are attributed to the presence/absence of ring strain at the adjacent α-carbon.

HINGE MOTION CAN BE OBSERVED

Hinge motion is reflected in variable temperature NMR spectra. Upon hinging, the positions of the substituents on the α-carbon of the amino acid undergo chemical exchange between pseudoequatorial and pseudoaxial environments. The methylenes labeled B and C behave similarly. Rapid exchange leads to coalescence. Decoalescence is observed at or above room temperature.

HINGE MOTION IS CONSERVED

Initially, macrocycles were obtained from quantitative cyclization reactions that employed trifluoroacetic acid. Variable temperature ^{1}H NMR spectra were recorded for each macrocycle *independently*. The results suggested that $\Delta G^{\ddagger}$ was similar across the series, establishing these molecules as choreoisosteres. The hinge barriers in DMSO-d_6 for **Acp**, **Aib**, and **Acb** were 14.6, 15.1, and 16.1 kcal/mol, respectively, with an error of ~0.2 kcal/mol. Because workup relied solely on evaporation of solvent (TFA:CH_2Cl_2), the amount of TFA could not be readily quantified. Furthermore, when the barrier for **Aib** was evaluated in different solvents, a marked difference was observed between organic solvents (CD_3OD, CD_3CN, Pyridine-d_5, DMSO-d_6; 15.0 ± 0.3 kcal/mol) and D_2O (15.9 ± 0.3 kcal/mol).[14]

To address these issues, cyclization was accomplished using difluoroacetic acid, allowing quantification of acid concen-

https://doi.org/10.1021/acsphyschemau.4c00103
ACS Phys. Chem Au 2025, 5, 134−138

tration by ^{1}H NMR. At similar acid concentrations, $\Delta G^{\ddagger}$ varied between 14.9 and 15.4 kcal/mol across these macrocycles.

^{13}C NMR SPECTROSCOPY SUCCESSFULLY REPORTS ON HINGE MOTION FOR A SAMPLE CONTAINING ALL THREE CHOREOISOSTERES

To confirm this conclusion, however, we sought to rule out environment effects that could derive from varying amounts of residual water in these samples. Accordingly, samples were generated from difluoroacetic acid and subsequently combined in a single NMR tube. The overlap of resonances in the ^{1}H NMR spectrum precluded evaluation using this nucleus. However, we posited that the data could be derived from variable temperature ^{13}C NMR spectroscopy. ^{13}C NMR spectroscopy has been explored for proteins and other biomolecules to probe gross conformational changes using solid-state samples.[15] Solution studies are far less common and largely limited to evaluating the barriers of rotation for single bonds, including those of triazines.[16]

Figure 4 shows the variable temperature NMR spectra collected at 100 MHz in DMSO-d_6. The colors identify

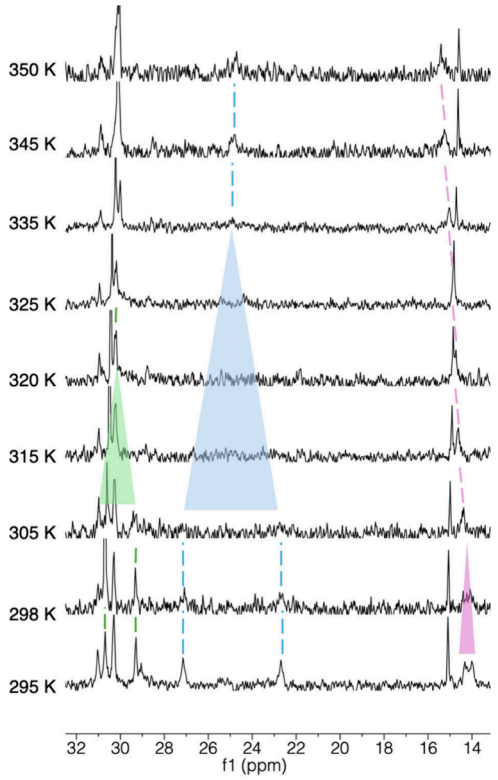

Figure 4. Variable-temperature ^{13}C NMR recorded at 100 MHz in DMSO-d_6 for the β-carbons of **Acb** (green), **Aib** (blue) and **Acp** (green). The shaded triangles indicate regions where spectral noise precludes definitive assessment.

coalescing resonances for β-carbons of the amino acid of each macrocycle; **Aib** (blue), **Acp** (purple), and **Acb** (green). Here, the triangles reflect the uncertainty in the evaluation of the data. That is, identifying the coalescence temperature, T_c, is made challenging by the sensitivity of the nucleus and the signal:noise ratio. Accordingly, we define a range bounded above by the temperature where the coalesced resonances are first observed and below at the temperature at which the decoalesced resonances are last observed. The magnitude of this range is consistent with the literature wherein ^{13}C spectra are often collected every 20 °C.[16] Resonances are rarely resolved over a narrow temperature range.[16f]

From the differences in chemical shift of the fully decoalesced resonances ($\Delta\nu$) and the coalescence temperature (T_c), the barrier for hinging ($\Delta G^{\ddagger}$) can be calculated by first calculating the rate of exchange (k_{exch}; eq 1), and subsequently solving the Eyring equation (eq 2) wherein, κ, the transmission coefficient, is assumed to be 1, h is the Planck constant, k_B is the Boltzmann constant, and R is the gas constant.[17]

$$k_{exch} = \pi(\Delta\nu)/\sqrt{2} \approx 2.22(\Delta\nu) \quad (1)$$

$$\Delta G^{\ddagger} = -RT_c\ln[(\kappa h k_{exch})/(k_B T_c)] \quad (2)$$

Using this strategy, the ranges of $\Delta G^{\ddagger}$ shown in Table 1 are in good agreement. The errors calculated do not exceed 0.2 kcal/mol. As expected, the rates for k_{exch} increase with increasing temperature, consistent with similar rates of hinging across the series. The values obtained are consistent with those values derived independently by ^{1}H NMR spectroscopy.

Table 1. Lower and upper bounds of T_c and corresponding range of $\Delta G^{\ddagger}$ as determined by variable-temperature ^{13}C NMR spectroscopy at 100 MHz in DMSO-d_6

Cmpd	T_c (lower)	T_c (upper)	$\Delta G^{\ddagger}$
Aib	315	335	14.2–15.1
Acp	295	305	14.7–15.2
Acb	310	320	14.6–15.1

ISOSTERISM ENABLES ADDITIONAL PREDICTION

The usefulness of the label "isostere" derives from predicting additional physical properties of a compound based on the known physical properties of an isostere. Langmuir's confidence in isosterism led him to predict similar structures for HCNO and HN_3 based solely on the observations that (*i*) both exploded upon heating and (*ii*) their potassium salts had crystallographic unit cells of similar dimensions.[1]

The predictive ability of bioisosterism is illustrated by the emergence of computational engines that link structure, bioactivity and physicochemical data.[18] These tools have advanced prediction from *classical* activities intended to conserve activity and physicochemical properties for lead optimization to *nonclassical* activities wherein entire fragments of molecules can be replaced to identify new lead compounds.

CHOREOISOSTERISM SUPPORTS CLASSICAL PREDICTIONS

To conclude these studies, we examined whether classical predictions pertaining to size and lipophilicity could be made for these molecules. Our expectation was that all three choreoisosteres would show similar metrics for these physicochemical properties. The results of these studies are shown in Table 2.

When the diffusion constants were measured simultaneously by an NMR DOSY experiment, the values were identical.[19]

Lipophilicity was assessed by measuring the octanol:water partition coefficients by RP HPLC at pH 9.0.[20] The modest increase in values is consistent with the increasing size of the hydrophobic substituent.

https://doi.org/10.1021/acsphyschemau.4c00103
ACS Phys. Chem Au 2025, 5, 134–138

Table 2. Common physical properties of choreoisosteres the log values of the partition coefficient (P) and permeability (P_e)[a]

Cmpd	logP	D	logP_e
Acp	0.3	0.7	−6.2
Aib	0.5	0.8	−6.1
Acb	1.0	1.5	−5.8

[a]Diffusion (D) is reported in $\times 10^6$ cm/sec.

Membrane transport for these macrocycles was evaluated by PAMPA.[21] A similar trend is observed for the diffusion constants (D). The values for logP_e (P_e is effective permeability) are markedly close to cyclosporin A (logP_e = −6.0), an orally available drug.

In conclusion, the pseudoatoms incorporated into **Aib**, **Acp**, and **Acb** are isosteric and lead to molecules that share common shape and dynamic behavior. This leads us to identify this isosterism more specifically as *choreoisosterism*. The predictive ability conveyed with choreoisosterism can offer insight into classical physicochemical properties as well as communicate the emergence of (or lack of any) new dynamic behavior arising from incongruous data.

We favor the prefix "*choreo*" because it connotes a molecular dance. Prefixes including "*dyna*" and "*mechano*" have been adopted elsewhere to describe phenomena unrelated to isosterism. *Dyna* has been employed to identify polymers derived from dynamic covalent or supramolecular chemistry.[22] *Mechano* can refer to reaction strategy[23] or a response in polymers to an external force.[24]

The extent to which choreoisosterism is demonstrated in other systems is unclear, and accordingly, the merits of introducing this unique moniker is a subject of debate. In potential contrast, examples of bioisosteres are pervasive. Assessing the extent of choreoisosterism in small molecules or supramolecular assemblies presents challenges given the lack of unifying nomenclature.

We have discovered examples of choreoisosteres in the dynamics of cyclohexane. In 1972, Lambert and co-workers examined ring flipping in cyclohexane rings with exocyclic methylenes, geminal dimethyl groups, and spiro-cyclopropyl groups.[25] The authors distinguished between the exocyclic methylene and the now-classic latter examples based on barriers to ring flipping. Moreover, the exocyclic methylene would not normally be considered isosteric. In a more recent example, Ye, Wang and co-workers reported that 1,6;2,3-bis-BN cyclohexane has similar ring-flip behavior to cyclohexane.[26,27]

Choreoisosterism could be envisioned to be demonstrated by supramolecular assemblies (*i.e.*, rotaxanes) or molecular machines, but examples wherein isosteric replacements led to conserved dynamics could not be identified from the literature.

An alternative to defining choreoisosterism with examples is to identify examples where it is absent. In this report, while **G** shows similar dynamic behavior as **Aib**, **Acp**, and **Acb**, CH_2 is neither an isostere of $C(CH_3)_2$ nor the spirocycles by either rigorous or pseudoatom definitions.[28] In addition, the barrier for hinge motion is notably lower. Similar distinctions can be made between the exocyclic methylene derivative of Lambert. Additionally, molecules displaying isosteric groups, but showing different structures and dynamics would not qualify as choreoisosteres.

As for the system reported here, additional choreoisosteres can be imagined. The substitution of triazine for pyridine or a related heterocycle is one example.[29] Replacing the hydrazone with an olefin is another. A third example, and less interesting perhaps, is the replacement of the auxiliary dimethylamine group with aziridine. Regardless, employing the descriptor *choreoisostere* affords on opportunity to efficiently convey a relationship between molecules that show isosteric structural connectivity: That is, these molecules display common dynamic behavior.

■ ASSOCIATED CONTENT

Supporting Information

The Supporting Information is available free of charge at https://pubs.acs.org/doi/10.1021/acsphyschemau.4c00103.

Synthetic details, NMR spectra, crystallographic data (PDF)

■ AUTHOR INFORMATION

Corresponding Author

Eric E. Simanek − *Department of Chemistry & Biochemistry, Texas Christian University, Fort Worth, Texas 76129, United States;* orcid.org/0000-0002-3195-4523; Email: e.simanek@tcu.edu

Authors

Alexander J. Menke − *Department of Chemistry & Biochemistry, Texas Christian University, Fort Worth, Texas 76129, United States;* orcid.org/0000-0001-9573-7045

Joseph H. Reibenspies − *Department of Chemistry, Texas A&M University, College Station, Texas 77843, United States*

Casey J. Patterson-Gardner − *Department of Chemistry & Biochemistry, Texas Christian University, Fort Worth, Texas 76129, United States;* orcid.org/0000-0002-0124-4117

Alexander M. Engstrom − *Department of Chemistry, University of California, Santa Cruz, California 95064, United States;* orcid.org/0000-0002-2364-5456

R. Scott Lokey − *Department of Chemistry, University of California, Santa Cruz, California 95064, United States;* orcid.org/0000-0001-9891-1248

Complete contact information is available at: https://pubs.acs.org/10.1021/acsphyschemau.4c00103

Author Contributions

All authors have given approval to the final version of the manuscript.

Funding

We thank the NIH (R15GM139950, EES; R35GM148282, RSL) and the Robert A. Welch Foundation (P-0008, EES) for support.

Notes

The authors declare no competing financial interest.

■ REFERENCES

(1) Langmuir, I. Isomorphism, Isosterism and Covalence. *J. Am. Chem. Soc.* **1919**, *41*, 1543−1559.

(2) Grimm, H. G. Structure and Size of the Non-metallic Hydrides. *Z. Electrochem.* **1925**, *31*, 474−480.

(3) Erlenmeyer, H.; Berger, E.; Leo, M. Relationships between the structure of antigens and the specificity of antibodies.V. *Helv. Chim. Acta* **1933**, *16*, 733−738.
(4) Friedman, H. L. Influence of isosteric replacements upon biological activity. *NAS-NRS Publication No. 206* **1951**, 295−358.
(5) Meanwell, N. A. The Influence of Bioisosteres in Drug Design:Tactical Applications to Address Developability Problems. In *Tactics in Contemporary Drug Design*; Meanwell, N. A., Ed.; Topics in Medicinal Chemistry; Springer: Berlin, Heidelberg, 2015; pp 283−381.
(6) Bauer, M. R.; Di Fruscia, P.; Lucas, S. C. C.; Michaelides, I. N.; Nelson, J. E.; Storer, R. I.; Whitehurst, B. C. Put a ring on it: application of small aliphatic rings in medicinal chemistry. *RSC Med. Chem.* **2021**, *12*, 448−471.
(7) The nomenclature adopted here deviates from our convention in that the names are truncated. **G-G** becomes **G**, etc.
(8) Capelli, R.; Menke, A. J.; Pan, H.; Janesko, B. G.; Simanek, E. E.; Pavan, G. M. Well-Tempered Metadynamics Simulations Predict the Structural and Dynamic Properties of a Chiral 24-Atom Macrocycle in Solution. *ACS Omega* **2022**, *7*, 30291−30296.
(9) Menke, A. J.; Mellberg, J. M.; Pan, H.; Reibenspies, J. H.; Janesko, B. G.; Simanek, E. E. Controlling Swing Rates in Macrocyclic Molecular Mortise Hinges. *Chem.-Eur. J.* **2023**, *29*, No. e202300987.
(10) Bold lines are used for rigid aromatic rings. Solid lines for bonds that show hindered rotation with barriers of 15−20 kcal/mol including the triazine-N bond and amide bond. Dashed lines show bonds between sp^3 hybridized atoms or sp^3-sp^2 bonds typically associated with low barriers to rotation. The impact of macrocyclization is not considered.
(11) Conservation of structure and dynamic behavior in triazine macrocycles with opportunities for subtle control of hinge motion. Patterson-Gardner, C. J.; Pan, H.; Janesko, B. G.; Simanek, E. E. *Org. Biomol. Chem.* **2025**, *23*, 1184.
(12) Inward orientation of carbonyls has been observed: Menke, A. J.; Gloor, C. J.; Claton, L. E.; Mekhail, M. A.; Pan, H.; Stewart, M. D.; Green, K. N.; Reibenspies, J. H.; Pavan, G. M.; Capelli, R.; Simanek, E. E. A Model for the Rapid Assessment of Solution Structures for 24-Atom Macrocycles: The Impact of β-Branched Amino Acids on Conformation. *J. Org. Chem.* **2023**, *88*, 2692−2702.
(13) Menke, A. J.; Henderson, N. C.; Kouretas, L. C.; Estenson, A. N.; Janesko, B. G.; Simanek, E. E. Computational and Experimental Evidence for Templated Macrocyclization: The Role of a Hydrogen Bond Network in the Quantitative Dimerization of 24-Atom Macrocycles. *Molecules* **2023**, *28*, 1144.
(14) For these studies, the samples were derived from the same solid material leading to the assumption that the ratios of trifluoroacetic acid to macrocycle were equivalent for each NMR sample, which were prepared at similar concentrations of sample.
(15) Beckman, N. *Carbon 13 NMR Spectroscopy of Biological Systems*; Academic Press, 1995.
(16) (a) Aitken, R. A.; Smith, M. H.; Wilson, H. S. Variable Temperature ^{1}H and ^{13}C NMR study of restricted rotation in N,N-bis(2-hydroxyethyl)acetamide. *J. Mol. Struct.* **2016**, *1113*, 171−175. (b) Mazzanti, A.; Boffa, M.; Marotta, E.; Mancinelli, M. Axial Chirality at the Boron−Carbon Bond: Synthesis, Stereodynamic Analysis, and Atropisomeric Resolution of 6-Aryl-5,6-dihydrodibenzo-[c,e][1,2]azaborinines. *J. Org. Chem.* **2019**, *84*, 12253−12258. (c) Sieh, D. H.; Wilbur, D. J.; Michejda, C. J. Preparation of Trialkyltriazenes. A Comparison ofthe N-N Bond Rotation in Trialkyltriazenes and Aryldialkyltriazenes by Variable Temperature ^{13}C NMR. *J. Am. Chem. Soc.* **1980**, *102*, 3883−3887. (d) Abraham, R. J.; Ribeiro, D. S. Conformational analysis. Part 36.1 A variable temperature ^{13}C NMR study of conformational equilibria in methyl substituted cycloalkanes. *J. Chem. Soc. Perkins Trans. 2* **2001**, 302−307. (e) Katritzky, A. R.; Ghiviriga, I.; Steel, P. J.; Oniciu, D. C. Restricted rotations in 4,6-bis and 2,4,6-tris-(N,N-dialkylamino)-s-triazines. *J. Chem. Soc. Perkin Trans. 2* **1996**, 443−447. (f) Katritzky, A. R.; Oniciu, D. C.; Ghiviriga, I.; Barcock, R. A. 4,6-bis- and 2,4,6-tris-N,N-dialkylamino)-s-triazines: synthesis, NMR spectra, and restricted rotations. *J. Chem. Soc., Perkin Trans. 2* **1995**, 785−792. (g) Rumjanek, V. M.; da Costa, J. B. N.; Echevarria, A.; Cavalcante, M. F. [^{13}C]Dynamic NMR and Molecular Modeling of 2,4-Bis(N-Pyrrolidinyl)-6-chloro-s-triazine. *Struct. Chem.* **2000**, *11*, 303−207.
(17) Casarini, D.; Lunazzi, L.; Mazzanti, A. Recent advances in stereodynamics and conformational analysis by dynamic NMR and theoretical calculations. *Eur. J. Org. Chem.* **2010**, *2010*, 2035−2056.
(18) Cuozzo, A.; Daina, A.; Perez, M. A. S.; Michielin, O.; Zoete, V. SwissBioisostere 2021: updated structural, bioactivity and physico-chemical data delivered by a reshaped web interface. *Nucleic Acids Res.* **2022**, *50*, D1382−D1390.
(19) (a) Johnson, C. S., Jr. Diffusion ordered nuclear magnetic resonance spectroscopy: principles and applications. *Prog. Nucl. Magn. Reson. Spectrosc.* **1999**, *34*, 203−256. (b) Evans, E.; Dal Poggetto, G.; Nilsson, M.; Morris, G. A. Improving the Interpretation of Small Molecule Diffusion Coefficients. *Anal. Chem.* **2018**, *90*, 3987−3994.
(20) Protonated macrocycles were too hydrophilic for the method employed: OECD (2022), *Test No. 117: Partition Coefficient (n-octanol/water), HPLC Method*, OECD Guidelines for the Testing of Chemicals, Section 1; OECD Publishing, Paris.
(21) (a) Kansy, M.; Senner, F.; Gubernator, K. Physicochemical High Throughput Screening: Parallel Artificial Membrane Permeation Assay in the Description of Passive Absorption Processes. *J. Med. Chem.* **1998**, *41* (7), 1007−1010. (b) Naylor, M. R.; Ly, A. M.; Handford, M. J.; Ramos, D. P.; Pye, C. R.; Furukawa, A.; Klein, V. G.; Noland, R. P.; Edmondson, Q.; Turmon, A. C.; Hewitt, W. M.; Schwochert, J.; Townsend, C. E.; Kelly, C. N.; Blanco, M.-J.; Lokey, R. S. Lipophilic Permeability Efficiency Reconciles the Opposing Roles of Lipophilicity in Membrane Permeability and Aqueous Solubility. *J. Med. Chem.* **2018**, *61*, 11169−11182.
(22) Roy, N.; Bruchmann, B.; Lehn, J.-M. DYNAMERS: dynamic polymers as self-healing materials. *Chem. Soc. Rev.* **2015**, *44*, 3786−3807.
(23) (a) Do, J. L.; Friscic, T. Mechanochemistry: A Force of Synthesis. *ACS Cent. Sci.* **2017**, *3*, 13−19. (b) James, S. L.; Adams, C. J.; Bolm, C.; Braga, D.; Collier, P.; Friscic, T.; Grepioni, F.; Harris, K. D. M.; Hyett, G.; Jones, W.; et al. Mechanochemistry: opportunities for new and cleaner synthesis. *Chem. Soc. Rev.* **2012**, *41*, 413−447. (c) Reynes, J. F.; Leon, F.; Garcia, F. Mechanochemistry for Organic and Inorganic Synthesis. *ACS Org. Inorg. Au* **2024**, *4*, 432−470.
(24) Zhang, H.; Diesendruck, C. E. Mechanochemical Diversity in Block Copolymers. *Chem.-Eur. J.* **2024**, *30*, No. e202402632.
(25) Lambert, J. B.; Gosnell, Jr. J. L.; Bailey, D. S. The Conformational Effect of the Spiro Linkage between three- and six-membered rings. *J. Org. Chem.* **1972**, *37*, 2814−2817.
(26) Dai, Y.; Zhang, X.; Liu, Y.; Yu, H.; Su, W.; Zhou, J.; Ye, Q.; Huang, Z. 1,6;2,3-Bis-BN Cyclohexane: Synthesis, Structure, and Hydrogen Release. *J. Am. Chem. Soc.* **2022**, *144*, 8434−843.
(27) 1,6;2,3-bis-BN cyclohexane has a backbone of (-CBNNBC-) wherein -BH_2 and -NH_2 groups are isosteres of -CH_2 groups of a cyclohexane backbone (-CCCCCC-).
(28) In the same light, using Langmuir's narrow definition, the cyclobutyl spirocycle of **Acb** is not rigorously an isomorphic substitution of the cyclopropyl or geminal dimethyl groups of **Acp** or **Aib**, but have been considered as such in other contexts (*ie* olefins). See, for example van der Kolk, M. R.; Janssen, M. A. C. H.; Rutjes, F. P. J. T.; Blanco-Ania, D. Cyclobutanes in Small-Molecule Drug Candidates. *ChemMedChem.* **2022**, *17*, No. e202200020.
(29) To this end, given the critical role that the protonated nitrogen plays in promoting the hydrogen bond network, only one of the three pyridine isomers would be expected to show similar structure and dynamic motion thereby qualifying as a choreoisostere.

https://doi.org/10.1021/acsphyschemau.4c00103
ACS Phys. Chem Au 2025, 5, 134−138